3-6 A continuous cellular automaton method with flux interpolation for two-dimensional electron gas electron transport analysis

Koichi Fukuda
AIST
Tsukuba, Japan
https://orcid.org/0000-0002-3148-6010

Junichi Hattori
AIST
Tsukuba, Japan

Hidehiro Asai
AIST
Tsukuba, Japan

Junya Yaita
Fujitsu Limited
Atsugi, Japan

Junji Kotani
Fujitsu Limited
Atsugi, Japan

***Abstract*— Due to the innovation of microwave communication using GaN-based HEMT, further improvement of HEMT device performance is expected. Prediction of transport properties of 2D electron gas is indispensable for designing HEMT devices. Since electron energy becomes high in HEMT channel because of its high electric field, a simulation method which covers the effects of band nonparabolicity, subband, and upper valley is required. By combining the Poisson-Schrodinger solver with the continuous cellular automaton method, a new simulation method is realized which stably obtains the electron distribution function over a wide range including the high-energy tail. It is reported that selfconsistent simulation is realized for the case where electron concentration redistribution by intersubband transitions affects subband energies through the Poisson-Schrodinger method.**

Keywords—GaN, HEMT, Poisson-Schrodinger, Cellular Automaton, device simulation, two-dimensional electron gas

I. INTRODUCTION

High electron mobility transistor (HEMT) is widely used as a high-power and high-speed device for microwave communication and is expected to be improved to higher performance [1][2]. Due to the innovation of microwave communication using GaN-based HEMT [3], further improvement of HEMT device performance is expected. The electron transport property of the two-dimensional electron gas formed by the energy barrier due to the heterolayer structure is the key to the high performance of HEMT. Therefore, it is important to predict the electron transport characterization in the two-dimensional electron gas 2DEG. Since the carrier energy increases due to the high acceleration electric field in the channel, the nonparabolicity of the energy band and the upper valley effect cannot be ignored.

A combination of the Poisson-Schrodinger method [4][5] and the Monte Carlo method [6][7] is often used to predict the electron transport properties of 2DEG [8][9]10]. In such approaches, the energy level and electron concentration profile of the subband are obtained by the Poisson-Schrodinger method, and the electron transport in the subband is obtained by the Monte Carlo method [11][12]. However, it is difficult for the method to consider the redistribution of electrons between subband and between valleys stably. Distribution function of electron over a wide energy range changes over many orders of magnitude cannot be efficiently obtained by the Monte Carlo method.

We propose the continuous cellular automaton method with the flux interpolation method [13] for this problem. This method calculates a continuous distribution function for orders of magnitude by introducing distribution function tables. The method reveals how the valley and the subband electron distribution changes over low to high electric fields and how the resulting carrier redistribution affects the subband energies in turn. The method clarified how the redistribution of carrier concentration affects the subband of HEMT. In the following chapter, the simulation method is de-scribed, and obtained 2DEG physics is discussed for a simple HEMT channel case.

II. SIMULATION METHOD

As shown in Fig. 1, the proposed method uses the Poisson-Schrodinger method to determine the subband and electron concentration distribution for the quantum confinement direction as z. Numerical tables for a two-dimensional wave vector space in the x and y directions are used for the distribution function representation for each subband. As an initial condition, the total amount of electron in each subband is obtained by the Poisson-Schrodinger method, and the energy distribution is set as thermal equilibrium.

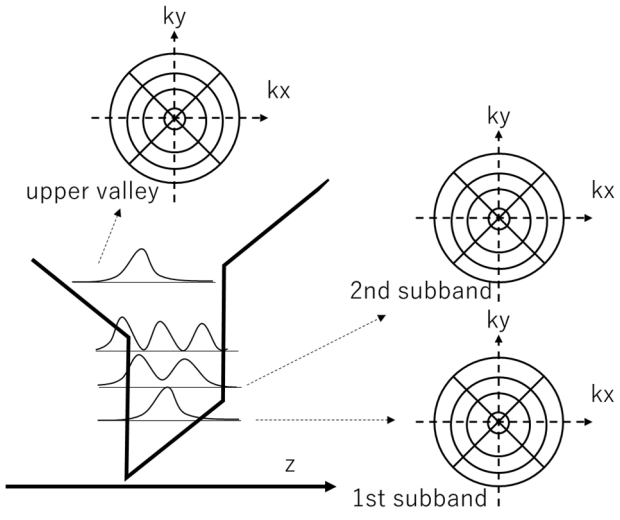

Fig. 1. Concepts of the proposed method. Distribution function tables for 2D momentum spaces are prepared for each subband and each valley obtained by Poisson-Schrodinger method.

As shown in Fig. 2, the cellular automaton method [13] is applied to update the distribution function at each time step. Since electrons are exchanged between valleys and subbands due to inter-valley and inter-subband scattering, the amount of

carriers in each subband changes. Since electron depth profiles are different between each subband, carrier exchanges between subbands cause electron profile redistribution. This affects the potential distribution through the Poisson equation, and it is necessary to solve the Poisson-Schrodinger method self-consistently. Because of the stable carrier distribution function obtained by the cellular automaton method, such effects can be accurately captured.

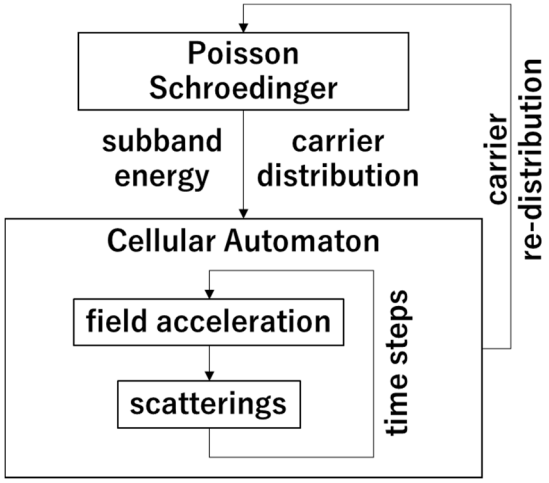

Fig. 2. Calculation flow of the proposed method. The distribution function tables are updated for each time step, according to the acceleration by the electric field and the scattering of various mechanisms. The distribution function updated by the cellular automaton method is used to update the carrier profiles, and is feed backed to Poisson-Schrodinger solver to consider the carrier redistribution effects.

Since the distribution function has wide orders of magnitude, a fine k-space mesh is required to suppress carrier pseudo-diffusion in the momentum space due to the large difference of values of the adjacent k-meshes when calculating fluxes at each time step. Fine k-meshes are not desirable because the calculation time of the method is significantly increased. For the k-space distribution function tables, logarithmic interpolation is assumed to calculate the flux which suppresses the pseudo diffusion problem with a reasonable number of k-meshes as conceptually explained in Fig. 3. The details are described in [13], which deals with the silicon as the bulk semiconductor case.

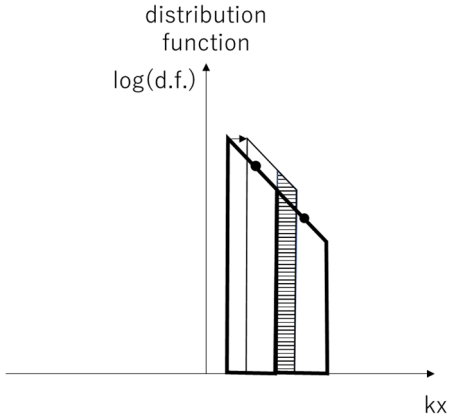

Fig. 3. One dimensional concept of the interpolation in the distribution function cell table. Each table covers a certain wave vector range shown by thick line box represented by a center point shown by black dot. When the representation point moved to the arrow direction, the distribution function flux is calculated as the hatched trapezoid. In the present method this scheme is applied to the 2D wave vector space.

For physical models of GaN-based HEMTs, electron scattering models from [14][15] and the model parameters from [16][17] are implemented into the present simulator. The heavy part of the simulation code is the cellular automaton loop and the loop is parallelized for distribution function tables by the OpenMP technology. For the top and the bottom boundary condition, a simple Schottky model is applied. The strain related interface charge is considered in the Poisson equation, which determine the electron charge area density for the equilibrium condition.

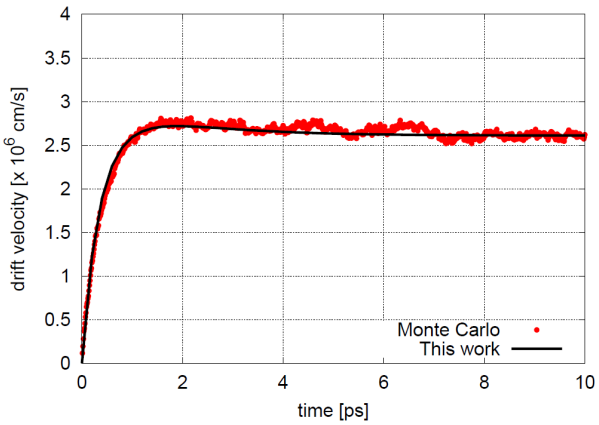

Fig. 4. Time dependent electron drift velocity after applying acceleration electric field of 1 kV/cm calculated by the present approach compared with the Monte Carlo results. In the Monte Carlo, 100,000 particles are used which is still not enough to reduce the fluctuation of the drift velocity.

Fig. 4 shows the transient electron drift velocity behavior after applying the low acceleration electric field of 1 kV/cm and is compared to the Monte Carlo method result using the same physical model. Assumed HEMT structure is AlN / GaN / AlN with 10 nm thickness for all three layers. Although for the Monte Carlo calculation, 100000 particles are used, the Monte Carlo results suffers such small fluctuations in the results since the random numbers are used to select scattering mechanisms. In the cellular automaton method, the amount of distribution function in each cell is divided and delivered to the final scattering condition in proportional to the each scattering mechanisms as schematically shown in Fig. 5.

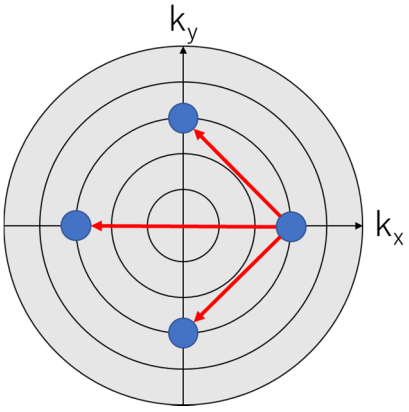

Fig. 5. The concept of the distribution function redistribution for each time step. The amount of the redistribution is calculated in proportional to the each scattering probability. This is the intra-subband and elastic scattering case, but same for inter-valley, inter-subband cases and for inelastic cases.

The final distribution function obtained for the same condition of Fig.4 is shown in Fig. 6. Thus, the distribution function obtained smoothly for wide, several tens orders of

magnitudes by the present method, which enables seamless analysis including high energy subbands and upper valleys. This feature plays an indispensable role especially for the high power III-V HEMTs with high voltage or hot carrier conditions.

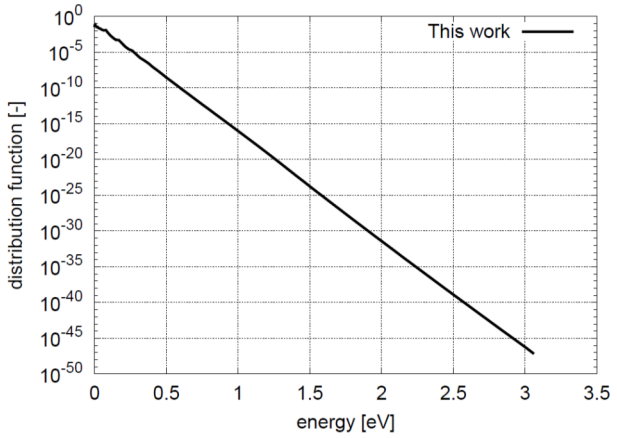

Fig. 6. The final distribution function obtained for the same low field condition of Fig. 4 calculation. The distribution function over wide orders of magnitude is smoothly obtained which enables seamless wide energy range analyses.

III. Simulation Results and Discussions

Fig. 7 shows the simple HEMT channel structure assumed as a test case for the proposed method. Both sides of the GaN channel layer are sandwiched by the barrier AlN layers. The z-axis in the figure is in the substrate depth direction which is the carrier confinement direction. The x-axis is assumed to be the horizontal direction to which the electron accelerating electric field is applied. When such an HEMT structure is analyzed, it is common to incorporate the interface charge due to the strain between different material layers caused by the lattice mismatch. The values of the interface charge assumed in this work are shown in the figure, which are rather high value corresponding to the large mismatch between pure AlN and GaN. It is worth mentioning that the program supports multiple layer structures in ordered to be used as the HEMT design tool.

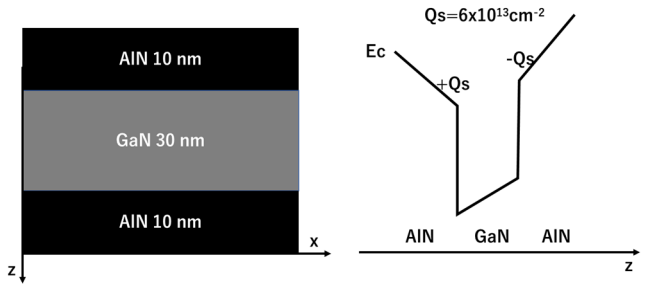

Fig. 7. Assumed device structure of GaN-based HEMT with strain induced charge assumed at semiconductor interfaces.

In GaN HEMT power applications, the acceleration electric field is large, so the carrier energy becomes high and it is necessary to consider the nonparabolicity of the electron energy band. The nonparabolicity affects not only the carrier transport but also the energy subband levels, and both are considered in the present simulation. Fig. 8 shows the band energy and the electron profiles for with and without the nonparabolicity consideration. There are clear differences in the subband energy levels and electron concentration distributions between the nonparabolic (red) and the parabolic energy band (blue). The nonparabolicity effectively increase the effective mass of higher energy subbands, which reduces the energy of the higher subband energy levels. As a results the carrier concentration is confined stronger by considering the nonparabolicity as shown in Fig. 8.

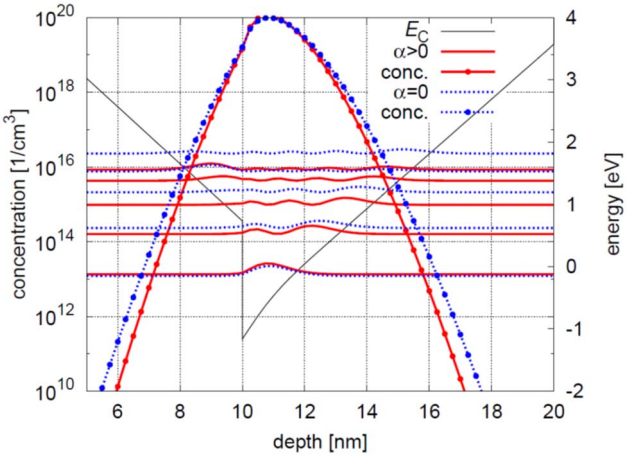

Fig. 8. Difference of subband (with marks) and electron concentration (lines) with (red) and without (blue) the nonparabolicity α consideration. The effective mass becomes heavier in higher energy, and the higher subbands energies reduced. This causes the stronger confinment which is considered by the present simulator.

Such carrier redistribution is also caused by applying large electric field. With high field, the electron energy becomes higher and the role of upper subbands or even upper valleys becomes significant. Electron depth profile differs depending on the subband levels which are determined by the confinement law of the Schrodinger equation. This means that the carrier profile is changed by applied acceleration fields. Fig. 9 shows the change of electron profile in the case of the large driving electric field of 500 kV/cm. Electron redistribution from the first to the upper subbands changes the electron profile wider, and the subband energies are affected by the redistribution in turn. It should be mentioned that these effects depend on the HEMT structures and band parameters.

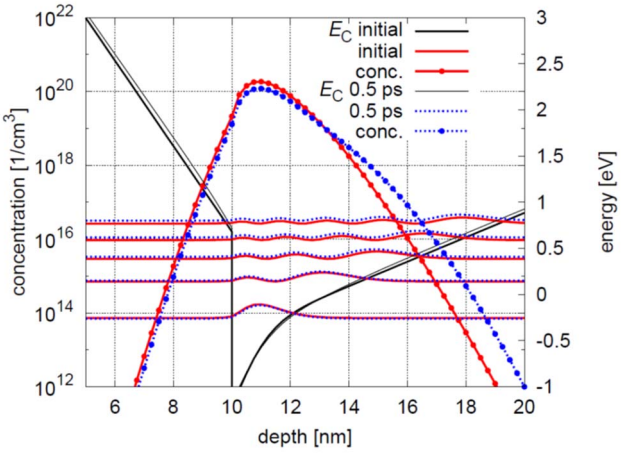

Fig. 9. Changes of subband energies and electron profile in the case of applied horizontal (x-direction) field of 500 kV/cm. Electron redistribution from the first to the upper subbands changes the electron profile with affects the subband energies in turn.

Fig. 10 shows the electron velocity overshoot characteristics for the condition of Fig. 9. Comparing to the overshoot in the low electric field in Fig. 4, the overshoot

under strong field is clearer and its time scale is shorter, which is often observed in the Monte Carlo analyses. It should be mentioned that the result contains the carrier redistribution effects especially after the overshoot. This overshoot result ensures that the obtained results incorporate the nonequilibrium effects of the Boltzmann transport equation as obtained by Monte Carlo method. The proposed method has additional merits in obtaining the distribution function stably for wide orders of magnitude regardless of the analysis conditions. This feature of the present method ensures the method to be a strong tool to design HEMTs, including the hot carrier effects important for power devices. Finally, it should be commented that the present approach incorporates the scattering mechanisms in proportional to their probabilities, and therefore does not cover the random nature of the carrier scattering which causes the noises by a finite number of electrons.

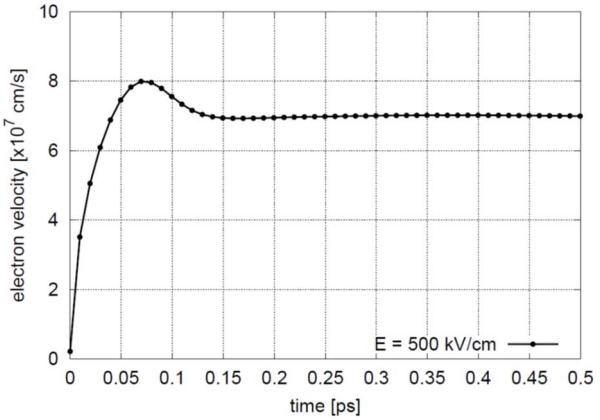

Fig. 10. Electron velocity overshoot characteristics for the same electric field condition of Fig.9. No comparison with the Monte carlo, because of the lack of the corresponding Monte Carlo code, coupled with Poisson-Schrodinger, with subbands and upper valley considerations. The overshoot is clearer than the low field condition in Fig. 4 and its time scale is shorter which are commonly observed in general Monte Carlo results.

IV. Conclusions

The continuous cellular automaton method coupled with the Poisson-Schrodinger method is proposed for the analysis of two-dimensional electron gas transport under high electric field. Since the carrier distribution function over a wide range is obtained stably and seamlessly, the method enables to investigate the effect of upper subbands and upper valleys on the electron transport, including the effect of carrier redistributions. It was confirmed through the test case of AlN-GaN HEMT structure, that the present method is a strong tool for carrier transport analysis of two-dimensional electron gas for wide range of electric field such as in HEMTs for power applications. In addition, the method is also a strong tool to design and optimize the HEMT layer structures based on the fundamental physics.

Acknowledgment

This work was partially supported by Innovative Sci-ence and Technology Initiative for Security Grant Number JPJ004596, ATLA, Japan.

References

[1] T. Mimura, “The early history of the high electron mobility transistor (HEMT),” IEEE Trans. Microw. Theory Tech., vol. 50, pp. 780-782, 2002.

[2] P. D. Ye, B. Yang, K. K. Ng, J. Bude, G. D. Wilk, S. Halder, and J. C. M. Hwang, “GaN metal-oxide-semiconductor high-electron-mobility-transistor with atomic layer deposited Al2O3 as gate dielectric,” Appl. Phys. Lett., vol. 86, no. 6, p. 063501, 2005.

[3] T. Ohki, A. Yamada, Y. Minoura, K. Makiyama, J. Kotani, S. Ozaki, and N. Nakamura, “An over 20-W/mm S-band InAlGaN/GaN HEMT with SiC/diamond-bonded heat spreader,” IEEE Electron Device Lett., vol. 40, no. 2, pp. 287-290, 2019.

[4] T. Ando, A. B. Fowler, and F. Stern, “Electronic properties of two-dimensional systems,” Rev. Mod. Phys., vol. 54, no. 2, pp. 437-672, 1982.

[5] C. Jacoboni and L. Reggiani, “The Monte Carlo method for the solution of charge transport in semiconductors with applications to covalent materials,” Rev. Mod. Phys., vol. 55, no. 3, pp. 645-705, 1983.

[6] W. Fawcett, A. D. Boardman, and S. Swain, “Monte Carlo ditermination of electron transport properties in gallium arsenide,” J. Phys. Chem. Solids, vol. 31, no. 9, pp. 1963-1990, 1970.

[7] S. E. Laux and F. Stern, “Electron states in narrow gate-induced channels in Si,” Appl. Phys. Lett., vol. 49, no. 2, pp. 91-93, 1986.

[8] P. Gorre, R. Vignesh, R. Arya, and S. Kumar, “A review of mm-wave power amplifiers for net-generation 5G communication,” Soft Computing: Theories and

[9] M.V. Fischetti and S. E. Laux, “Monte Carlo study of electron transport in silicon inversion layers,” Phys. Rev. B, vol. 48, no. 4, pp. 2244-2274, 1993.

[10] C. Jngemann, A. Emunds, and W. L. Engl, “Simulation of linear and nonlinear electron transport in homogeneous silicon inversion layers,” Solid-State Electron., vol. 36, no. 11, pp. 1529-1540, 1993..

[11] J. L. Thobel, L. Baudry, P. Bourel, F. Dessenne, and M. Charef, “Monte Carlo modeling of high-field transport in III-V heterostructures,” J. Appl. Phys., vol. 74, no. 10, pp. 6274-6280, 1993.

[12] J. Fang, M. V. Fischetti, R. D. Schrimpf, R. A. Reed, E. Bellotti, and S. T. Pantelides, “Electron transport properties of $Al_xGa_{1-x}N$/GaN transistors based on first-principles calculations and Boltzmann-equation Monte Carlo simulations,” Phys. Rev. Appl., vol. 11, no. 4, p. 044045, 2019.

[13] K. Fukuda and K. Nishi, “An interpolated flux scheme for cellular automaton device simulation,” IEEE Trans. CAD, vol. 17, no. 7, pp. 553-560, 1998.

[14] H. Tanimoto, N. Yasuda, K. Taniguchi, and C. Hamaguchi, “Monte Carlo study of hot electron transport in quantum wells,” Jpn. J. Appl. Phys., vol. 27, no. 4R, pp. 563-571, 1988.

[15] S. Yamakawa, E. Ueno, K. Taniguchi, C. Hamaguchi, K. Miyatsuji, K. Masaki, and U. Ravaioli, “Study of interface roughness dependence of electron mobility in Si inversion layers using the Monte Carlo method,” J. Appl. Phys., vol. 79, no. 2, pp. 911-916, 1996.

[16] B. E. Foutz, S. K. O’Leary, M. S. Shur, and L. F. Eastman, “Transient electron transport in wurtzite GaN, InN, and AlN,” J. Appl. Phys., vol. 85, no. 11, pp. 7727-7734, 1999.

[17] M. Farahmand, C. Garetto, E. Bellotti, K.F. Brennan, M. Goano, E. Ghillino, and. P. P. Ruda, “Monte Carlo simulation of electron transport in the III-nitride wurtzite phase materials system: binaries and ternaries,” IEEE Trans. Electron Devices, vol. 48, no. 3, pp. 535-542, 2001.